Phys. Biol. **8** (2011) 066006 (9pp) doi:10.1088/1478-3975/8/6/066006

Quantitative analysis of the ion-dependent folding stability of DNA triplexes

Gengsheng Chen and Shi-Jie Chen[1]

Department of Physics and Astronomy and Department of Biochemistry, University of Missouri, Columbia, MO 65211, USA

E-mail: chenshi@missouri.edu

Received 17 August 2011
Accepted for publication 13 October 2011
Published 9 November 2011
Online at stacks.iop.org/PhysBio/8/066006

Abstract

A DNA triplex is formed through binding of a third strand to the major groove of a duplex. Due to the high charge density of a DNA triplex, metal ions are critical for its stability. We recently developed the tightly bound ion (TBI) model for ion–nucleic acids interactions. The model accounts for the potential correlation and fluctuations of the ion distribution. We now apply the TBI model to analyze the ion dependence of the thermodynamic stability for DNA triplexes. We focus on two experimentally studied systems: a 24-base DNA triplex and a pair of interacting 14-base triplexes. Our theoretical calculations for the number of bound ions indicate that the TBI model provides improved predictions for the number of bound ions than the classical Poisson–Boltzmann (PB) equation. The improvement is more significant for a triplex, which has a higher charge density than a duplex. This is possibly due to the higher ion concentration around the triplex and hence a stronger ion correlation effect for a triplex. In addition, our analysis for the free energy landscape for a pair of 14-mer triplexes immersed in an ionic solution shows that divalent ions could induce an attractive force between the triplexes. Furthermore, we investigate how the protonated cytosines in the triplexes affect the stability of the triplex helices.

S Online supplementary data available from stacks.iop.org/PhysBio/8/066006/mmedia

Introduction

A DNA triple helix (tsDNA) is formed by a third strand binding to the major groove of a DNA duplex (dsDNA) through hydrogen bonds (Hoogsteen or reverse Hoogsteen base pairing) [1]. The naturally occurring intra-molecular triplexes play an important role in gene regulation and DNA repair [2]. Gene transcription requires unwinding of DNA helix. If a DNA triplex is formed, the high stability of the triplex may prohibit the unwinding of the helix, resulting in inhibition of transcription. Based on the functional relationship between triplex formation and gene regulation, therapeutic strategies have been proposed to design specific oligonucleotides to bind to DNA duplex and form triplexes. A theory that can predict triplex stability would be essential for quantitative understanding of triplex function and rational design of triplex-based therapeutic strategies.

In a DNA triplex, three polyanionic strands are in close contact, causing a high charge density of the structure [3]. Such a high charge density would draw a significant amount of counterions in the solution. Therefore, ion-mediated electrostatic interactions can be significant for triplex stability and ions are critical for triplex stability [4–6].

Recently, Bai *et al* [7] used buffer equilibration and atomic emission spectroscopy (BE-AES) to quantify the cation association and anion depletion for the DNA duplex and triplex. A comparison between the BE-AES data and the predictions from the Poisson–Boltzmann (PB) theory showed a notable discrepancy for the number of bound ions for the triplex and the theory–experiment difference is larger for a triplex than for a duplex. The surface charge density, which is 40% higher for a triplex than duplex, would result in a higher concentration of bound ions and thus possibly stronger correlation between the bound ions. This may cause a larger

[1] Author to whom any correspondence should be addressed.

inaccuracy in the PB predictions, which ignore the correlation effect.

Ions show intriguing behaviors in mediating the interactions between the different DNA duplexes and triplexes. Highly charged DNA helices tend to repel each other. However, experimental findings show that trivalent ions can effectively condense DNA duplex at micromolar concentrations [8]. In contrast, monovalent and divalent cations do not condense dsDNA even at molar concentrations [8]. For triplexes, using small angle x-ray diffraction, Qiu *et al* [9] recently observed divalent counterion-induced condensation of triple-stranded DNAs even in micromolar concentrations. In the current study, using the recently developed tightly bound ion (TBI) model [11–13], which can account for the ion fluctuation as well as the possible correlation effects, we calculate the free energy landscape for a pair of 14-base triplexes to investigate how multivalent ions mediate the force between two triplexes.

Experimental studies have also shown that the stability of DNA triplexes is strongly dependent on the sequence. For the Y·RY triplex (Y = pyrimidine: C or T; R = purine: A or G), the electrostatic potential of the protonated cytosines (if Y = C) in the third strand could cause highly complex electrostatic effects. Several experimental studies show that the C^+·GC triplex is much more stable than the T·AT triplex at a low pH value [10]. Experimental evidence also shows that the number of protonated cytosines affects the stability of the C^+·GC triple helices [10]. Recently, James *et al* [10] used oligonucleotides which contain fluorophores and quenchers to measure the stability of four 15-mer intermolecular triplexes with a third strand containing repeating TTT (CTTTTTTTTTTTTTT), CTT (CTTCTTTCTTCTTCT), CCT (CTCTCCTCCTCCTCC) and CTCT (CTCTCTCTTCTCTCT) sequences, respectively. It was found that the triplexes with repeating TTC, TCC and CTCT are much more stable than the T·AT triplex. The most stable triplex is for a sequence containing alternate C^+·GC and T·AT triplets. All of the triplexes are stabilized by increasing the ionic strength. However, triplexes with a higher proportion of C^+·GC triplets are much less sensitive to the changes in the ionic conditions.

In this study, we will first investigate the ion-dependent stability for a experimentally studied system: a 24-base triplex (CTCTTCTTTCTTTCTCCTCCTTTT). We will then compute the distribution of the ion atmosphere surrounding the triplexes and examine how ions mediate charge–charge interactions that stabilize the triplexes. We will also predict the free energy landscape for a pair of 14-base triplexes and examine the effect of the strand length and ion concentration on the folding stability. Furthermore, we will investigate how the protonated cytosines affect the stability of the triplex helices.

Methods

Structural model

In the following steps, we will show how to construct the three-dimensional structures of the DNA triplexes of lengths 8-base, 14-base, 15-base and 24-base. The construction of the three-dimensional structures of the DNA triplexes involves the following steps. We use the experimentally determined 8-base triplex structure (TCTCTCTT, PDB code: 1D3X) as the building block for the construction of other triplex structures. In order to generate the 14-base triplexes, we first build 16-base triplexes by coaxially stacking two of the 8-base DNA triplexes. To join the two 8-base triplexes, we let the C_1, C_4, N_1 (for C and T) or N_9 (for A and G) coordinates in three terminal nucleotides of the joining triplexes to overlap. We then assemble the backbone chain of the helix stems using the least-squares fit between the two sets of atoms [14]. By deleting two redundant base triplets in the 16-base triplex, we obtain the atomic structures of the 14-base triplexes. Using the same method, we construct the atomic structure for a 24-base triplex from three coaxially stacked 8-base DNA triplexes. We can also build the atomic structure of a 15-base triplex from several coaxially stacked short DNA triplexes following the specific sequence of the nucleotides.

An extended TBI model for the DNA triplex

The previous TBI model was developed for polyanionic nucleic acid structures. Here we extend the TBI model to treat triplexes which could also contain positive charges in the third strand due to prontonation.

For a Y·RY triplex, the electrostatic potential produced by the protonated cytosines in the third strand makes it more complicated to analyze the cation effects. Several studies show that the Y·RY triplex has a greater stability than T·AT. This effect may come from the positive charges on the C^+s, which can compensate the repulsive interactions between the negative charges on the phosphates.

For a given conformation of the DNA triplex immersed in the salt solution, we solve the nonlinear PB equation to obtain the ion distribution $c(r)$. From $c(r)$, we determine the tightly bound region, which is defined as the region where the Coulombic correlation between the ions is strong, or the ions are so crowded that they start to bump into each other [11]. The tightly bound region is usually a thin layer around RNA. We use the TBI model to treat the TBI region and use PB to treat the rest (weakly correlated) ions.

For an N nt triplex, we divide the tightly bound region into N cells, each around a phosphate. We then discretize the ion distribution according to the number of ions in each cell. A given distribution of the TBIs is called a binding mode. To calculate the total free energy, we need to include the Coulombic interaction energy between all the protonated cytosines and between the protonated cytosines and the phosphates (including the bound ions). We calculate the pair potentials of mean force for the protonated cytosines and the phosphates. The results are tabulated for the calculations of the partition function. The partition function for a given binding mode M is

$$Z_M = Z^{(id)} \left(\frac{N_z}{V}\right)^{N_b} \times \left(\int \prod_{i=1}^{N_b} \mathrm{d}\mathbf{R}_i\right) \mathrm{e}^{-(\Delta G_b + \Delta G_d + \Delta G_b^{\mathrm{pol}} + \Delta G_{cc} + \Delta G_{cp})/k_B T}, \quad (1)$$

where N_b is the number of the TBIs for model M and $Z^{(id)}$ is the partition function for the uniform ion solution (without the nucleic acid). N_z and V are the total number of multivalent ions and the volume of the solution. $\int \prod_{i=1}^{N_b} \mathrm{d}\mathbf{R}_i$ is the volume integral for the N_b TBIs. ΔG_b is the Coulombic interaction energy between all the discrete charge–charge pairs (including the negatively charged phosphates and the N_b positively charged TBIs) within the tightly bound region; ΔG_d is the free energy for the diffusive ions, including the interaction energy between the diffusive ions and the charges in the tightly bound region (phosphates and TBIs). $\Delta G_b^{\mathrm{pol}}$ is the (Born) self-polarization energy for the discrete charges within the tightly bound region [15]. ΔG_{cc} is the Coulombic interaction energy between the protonated cytosines and ΔG_{cp} is the Coulombic interaction energy between the protonated cytosines and the phosphates (including the binding ions):

$$\Delta G_{cp} = \sum_{ij} \Phi_{cp}(i, j). \tag{2}$$

Here $\Phi_{cp}(i, j)$ is the pairwise potential of mean force (PMF),

$$\Phi_{cp}(i, j) = -k_B T \ln\langle \mathrm{e}^{-u_{ij}/k_B T}\rangle, \tag{3}$$

u_{ij} is the Coulombic interaction between the cytosines i and phosphates j. We use the generalized Born (GB) model to calculate the Coulomb interactions u_{ij} for charges in the cytosines i and phosphate j. The Coulombic interactions between the cytosines i and j are calculated from the following equation:

$$\Delta G_{cc} = \sum_i \sum_{j>i} \frac{e^2}{\epsilon_p r_{i,j}}. \tag{4}$$

Here ϵ_p is 20. For pH = 5.0 (experimental condition in [10]) and pKa = 0.45 for a DNA triplex [16], we assume the average probability of protonation to be 0.24 (from $\mathrm{pH}-\mathrm{pKa} = \log[\mathrm{A}^-]/[\mathrm{AH}]$). Averaging over the different binding modes gives the electrostatic free energy G^{el} of the system:

$$G^{\mathrm{el}} = -k_B T \ln \sum_M \left(Z_M / Z^{(id)}\right). \tag{5}$$

From equation (5), we calculate the electrostatic free energy and the comparison with the experimental results.

Results and discussions

Ion binding to 24-base DNA triple helices: Na^+–Mg^{2+} competition

In the TBI model, the bound ions of a DNA include both the TBIs and the diffusively bound ions (in the excess of bulk concentrations). We calculate the total number of bound ions from the following equation:

$$N_{\mathrm{total}} = N_{\mathrm{tbi}} + \int [c(\vec{r}) - c_0]\, \mathrm{d}^3\vec{r}. \tag{6}$$

Here N_{tbi} is the total number of the TBIs, which is calculated from the ensemble average over all the possible ion-binding modes:

$$N_{\mathrm{tbi}} = \sum_M N_b Z_M / Z, \tag{7}$$

where N_b is the number of the TBIs for mode M, Z_M is the partition function of the system in mode M, see equation (1), and $Z = \sum_M Z_M$ is the total partition function. The second term in equation (6) is the contribution from the diffusively bound ions, where $c(\vec{r})$ and c_0 are the ion concentrations at $\vec{r}$ and the bulk concentration, respectively.

As shown in figure 1, for a wide range of $[Na^+]$ and $[Mg^{2+}]$, the theoretical predictions show good agreement with the experimental data. The results lead to the following major conclusions.

(1) Metal ions are critical for triplex stability and the roles of Na^+ and Mg^{2+} ions are anti-cooperative (see figure 1(*A*)). With the increase of the Mg^{2+} concentration, the number of Mg^{2+} bound ions is increased, while the number of Na^+ bound ions is decreased (see figure 1(*B*)). For Na^+ competes with 5 mM Mg^{2+} background, for low $[Na^+]$, Mg^{2+}-binding is dominant due to the strong Mg^{2+}-phosphate attraction and the low entropy penalty for Mg^{2+} binding, and Na^+-binding is suppressed. With the addition of Na^+, for a sufficiently high $[Na^+]$, Mg^{2+} binding is replaced with Na^+ binding, and Na^+ ions dominate the triplex stability. Similar behavior is also evident for Mg^{2+} competes with 20 mM Na^+ background as shown in the figure.

(2) PB underestimates the number of Mg^{2+} ions bound to the helix and overestimates the number of bound ions for Na^+. This is due to the neglect of the ion correlation in the PB calculation, which leads to underestimation of Mg^{2+} ion binding and hence an overestimation of Na^+ ion binding. In contrast, the TBI model gives much improved predictions than PB for the number of bound ions.

Comparison of ion binding properties: triplex versus duplex

In this section, to compare the ion binding properties for a triplex and duplex, we calculate the number of bound ions around a 24-base DNA duplex and a 24-base DNA triplex using PB and the TBI model and compare the theoretical predictions with the experimental data. The results are shown as follows.

As we expect, more ions bind to the triplex than to the duplex (see figure 2) due to the higher charge density of the triplex than duplex. In addition, the overall theoretical predictions from our TBI model agree with the experimental data. The TBI model gives improved predictions than the PB theory. The observed deviations between the PB calculation and the experimental data are larger for the triplex than for duplex, which suggests that ion correlation may be more important for a complex structure such as a triplex than for a simple structure such as a duplex (see figure 3). This is because the higher charge density of a triplex (than a duplex) causes stronger ion binding and higher concentration of bound ions around the helix, resulting in stronger correlation between the ions.

Free energy landscape for a pair of 14-base triplexes

Understanding the force between highly charged DNAs/RNAs has significant implications in biology. In this section, in order

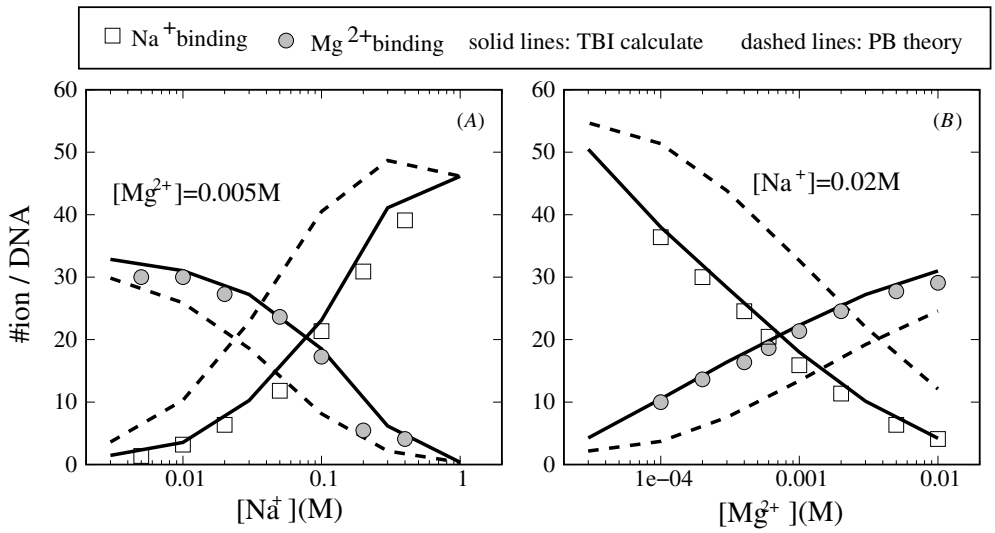

Figure 1. Competitive association of Na^+ and Mg^{2+} with the 24-base DNA triplex (T24 L). The symbols represent the experimental data [7]. The solid lines are calculated from the TBI model, and the dashed lines are calculated from the PB theory. (*A*) Na^+ (square) competes with 5 mM Mg^{2+} background (circle). The downturn of the dashed line at high [Na^+] may be caused by numerical error. (*B*) Mg^{2+} (circle) competes with 20 mM Na^+ background (square).

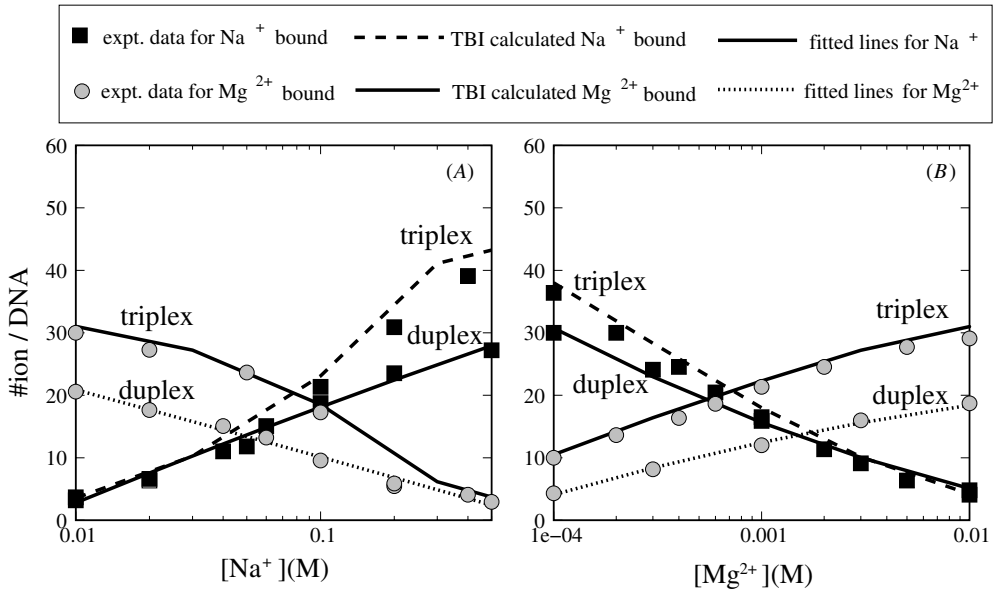

Figure 2. Competitive association of Na^+ and Mg^{2+} with the 24-base DNA triplex (T24 L). The symbols represent the experimental data [7]. The solid and dashed lines (for triplex) are calculated from the TBI model, and the other lines (for duplex) are fitted from experimental data. (*A*) Na^+ (square) competes with 5 mM Mg^{2+} background (circle). (*B*) Mg^{2+} (circle) competes with 20 mM Na^+ background (square).

to investigate the effects of divalent ions in the condensation of triple helix, we investigate the electrostatic free energy landscape for a pair of 14-base triplexes (see figure 4) and examine the effects of the ionic strength on the electrostatic free energy landscape of the system. Here, the electrostatic free energy landscape is the electrostatic free energy as a function of the spatial configuration of the system.

For the system of a pair of 14-base triplexes, we depict the free energy landscape using the angles (θ, β) and the distance between the triplexes; see figure 5. To calculate the electrostatic free energy landscape $G^{\rm el}(\theta, x)$, we change the θ angle from 0° to 180° with a 20° step size, and the distance x from 22 to 60 Å with a 2 Å step size. For each given θ and x, we use the TBI theory to calculate the electrostatic free energy $G^{\rm el}(\theta, x)$ for two different β angles. To investigate how ions affect the free energy landscape, we calculate $G^{\rm el}(\theta, x)$ for the different ion conditions. Our results lead to the following conclusions.

(1) Divalent cations can condense tsDNA at millimolar concentration (see figures 4(*A*) and (*B*)), which is consistent with the experimental finding [9]. For the DNA triplex, the charge density is very high (about 40% higher than ds-DNA), more ions become tightly bound in response to the enhanced electric field, causing a stronger correlation between the TBIs distributed between

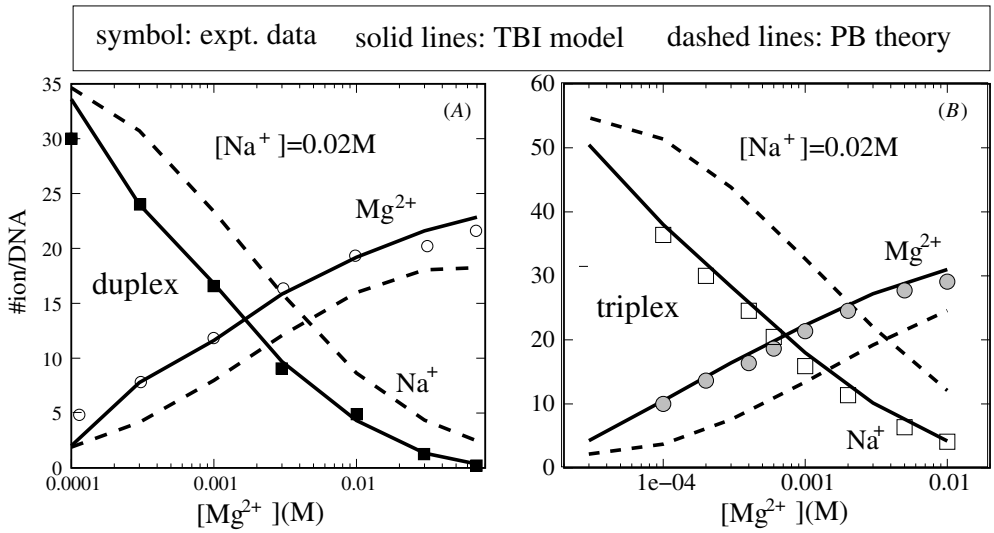

Figure 3. Competitive association of Na^+ and Mg^{2+} with the 24-base DNA duplex. The symbols represent the experimental data [7]. The solid lines are calculated from the TBI model, and the dashed lines are calculated from the PB theory. (*A*) 24-base DNA triplex and (*B*) Mg^{2+} (circle) compete with 20 mM Na^+ background (square).

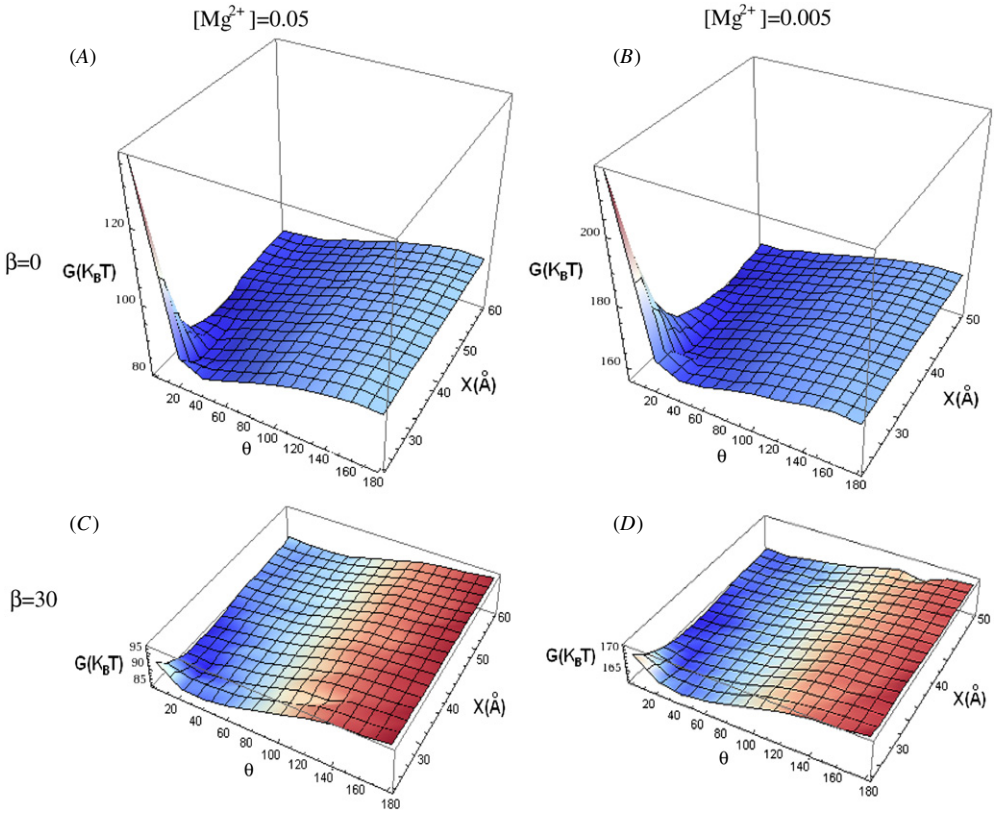

Figure 4. The three-dimensional plot for the electrostatic free energy landscapes (in k_BT) for a pair of 14-base triplexes at different $[Mg^{2+}]$ concentrations. (*A*) and (*C*) $[Mg^{2+}] = 0.05$ M, (*B*) and (*D*) $[Mg^{2+}] = 0.005$ M. The *x*-axis (θ) represents the inter-axis angles between two 14-base triplexes and the *y*-axis represents the distances between the ends of these two triplexes; see figure 5. The *z*-axis shows the electrostatic free energy.

the helices. The correlated ions can self-organize to reach correlated low-free energy configurations. Such correlated states can reach much lower energies than the (uncorrelated) mean-field states. In addition, as the helices approach each other, more ions become tightly bound and hence the correlation effect becomes stronger, resulting in an attraction between the triplexes. For two parallel DNA helices, the inter-helix attractive force is strongest (see the free energy minima at $\theta = 0^\circ$ in figure 4). For very closely packed helices, the finite size of the ions would reduce the probability for ions to distribute between the helices. As a result, the parallel helices would

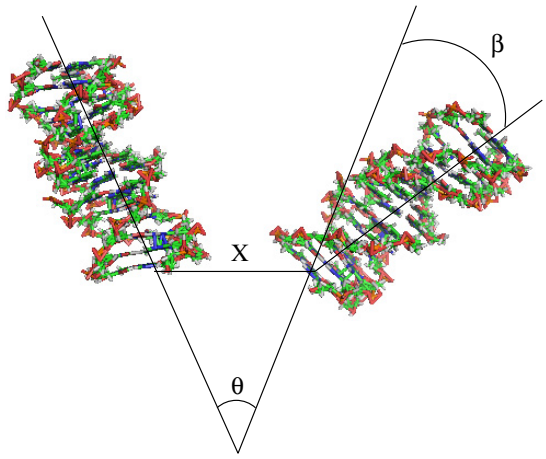

Figure 5. Illustration of the structure parameters.

repel each other due to the Coulombic repulsions between helices, resulting in a high free energy for small x and θ; see figures 4(A) and (B).

(2) The attraction between two helices increases with the increase of ion concentration (see figures 4(A) and (B)). This is because a higher [Mg^{2+}] causes more bound ions and hence a lower electrostatic free energy and stronger helix–helix attraction (shown by a lower free energy minima for figure 4(A) than for (B)), and hence a more compact state (shown by the shift of the free energy minima from figure 4(A) to (B)).

(3) The attraction between the triplexes varies with the different orientations of the two helices (see figure 4). The attraction force is stronger for coplanar than non-planar triplexes. The planar structure generally involves a higher overall charge density of the system and stronger electrostatic interactions, resulting in a stronger correlation effect and attractive force between the helices than non-planar structures.

Distribution of the TBIs

Motivated by the importance of ionic environment to intermolecular interactions and structural stability, we have also investigated the ion distribution around triplexes for the above triplex pair. Specifically, we calculated changes of the Mg^{2+} ion distribution as the two triplexes approach each other for six representative conformations as characterized by the θ and x parameters; see figure 6.

In the TBI model, the fraction of the tightly bound Mg^{2+} ions per nucleotide is given by the average over all the possible binding modes M of the TBIs:

$$f_b = \frac{1}{2NZ}\sum_M N_b Z_M, \tag{8}$$

where N_b is the number of the TBIs for mode M, Z_M is the partition function of the system in mode M, Z is the total partition function and N is the number of the phosphates on each strand. The charge distribution shows that

(1) For a large helix–helix separation, the distribution of the bound ions on the different helices is nearly independent of each other and the inter-helix correlation is weak. Most Mg^{2+} ions tend to bind at the middle of helix and less Mg^{2+} ions binding at the helix ends (see figure 6). Generally, the middle region of the helix has a higher charge density of the backbone phosphate charges than the ends and thus attracts more TBIs. In contrast, the helix ends have relatively lower phosphate charge density and hence weak electric field and less TBIs [15]. Such an end-effect is manifested as weaker charge neutralization at the helix ends.

(2) The approach of two helices causes an increasing number of the TBIs due to the increased phosphate charge density of the two helices (see figure 6). The change in the charge density of the triplex DNA system results in the change in the electric field which renders the changes in the counterion distribution.

Physically, when the two helices approach each other, more ions become tightly bound in response to the enhanced electric field, causing a stronger correlation between the TBIs on the different helices. The correlated ions can self-organize to form the correlated low-energy states. In the correlated low-energy states, the bound ions tend to reside in the region of the lowest electric potential produced by all the bound and the diffusive ions as well as the phosphates on both helices. From figures 6(B), (C), (E) and (F), which show the most probable low-energy binding modes, we find that the strongest correlation occurs between ions bound to phosphates that are directly facing each other. To more efficiently lower the energy, ions have higher tendency to bind to these phosphates where the ions are highly correlated. The most probable binding mode gives a strong attractive force. The ensemble-averaged, mean-binding mode indicates that ions prefer to bind to the region between the two helices so as to interact with both helices strongly.

Temperature dependences of the inter-axial spacings between two parallel tsDNAs

In this section, we investigate the mean equilibrium helix–helix distance $\bar{x}$ under different temperatures for the different triplex length. The mean equilibrium helix–helix distance $\bar{x}$ is computed as

$$\bar{x} = \frac{\sum x\, \mathrm{e}^{-G(x)/k_BT}}{\sum \mathrm{e}^{-G(x)/k_BT}}. \tag{9}$$

Here $G(x)$ is the electrostatic free energy for the structure when the inter-axial spacing of two parallel tsDNA is x. For each temperature, we change the distance x from 22 to 60 Å with a 2 Å step size. The calculated results lead to the following conclusions.

First, the TBI-predicted trend for the change of the inter-axis distance as a function of the temperature agrees well with the experimental results. Since our current TBI model can only treat a DNA/RNA of length less than 84 nt, we can only

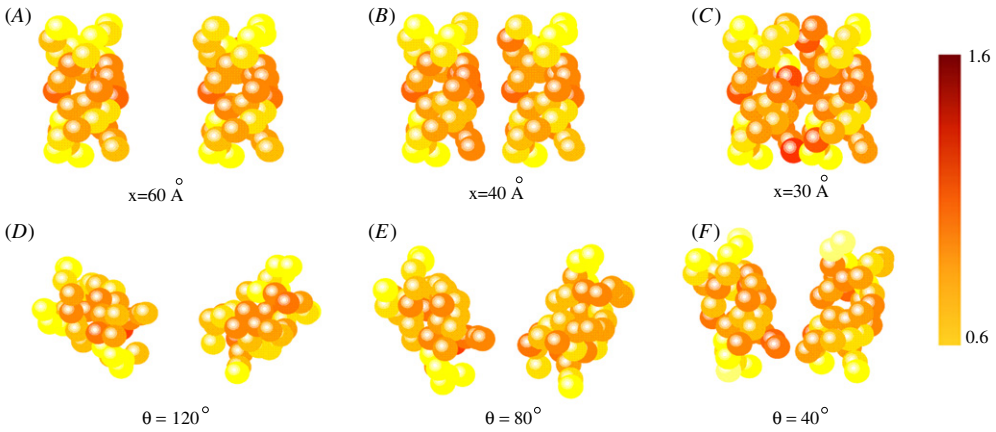

Figure 6. Distribution of the tightly bound Mg^{2+} ions for the states with $x = 30$, 40 and 60 Å and $\theta = 40^\circ$, 80° and 120° in 0.05 M Mg^{2+}. The spheres with color changing from dark to light represent phosphates with strong to weak charge neutralization, i.e. more ions are found around the dark color spheres than around the lighter color spheres.

treat a pair of triplexes with each helix not longer than 14-base. As a result, we can only treat triplexes shorter than the ones studied in the experiments and compare the trend of the temperature dependence of the inter-helix distance.

Second, the inter-axis spacing decreases with the increase of temperature (see figure 7). In our calculation, such a temperature dependence comes from the effect of the solvent dielectric constant:

$$\varepsilon(t) = 87.740 - (0.4008)t + (9.398 \times 10^{-4})t^2 - (1.41 \times 10^{-6})t^3, \quad (10)$$

where t is the temperature in celsius. With the increase of the temperature, the dielectric constant decreases, which weakens the dielectric screening of the solvent. A lower dielectric screening causes stronger charge–charge interaction and ion–helix binding. As a result, a smaller ε leads to more bound ions and hence stronger ion-correlation, causing a stronger attraction and closer approach between the triplexes.

Sequence-dependent stability of the DNA triplex

The ion dependence of triplex stability is sequence dependent [10]. One of the sources to cause the sequence effect is the protonation of the cytosines in the third strand. Protonation state of the triplex can cause complex electrostatic effects due to the highly charged structure with mixed positive and negative charges and their interactions with the ionic environment. In this section, we investigate the electrostatic free energies for the different triplexes with the different sequence contexts and compare the theoretical predictions with the experimentally determined sequence-dependent melting temperature; see figure 8. As a caveat, we note that due to the unavailability of the single-strand DNA structure or structural distribution, which is required for the calculation of the melting temperature, we cannot calculate the melting temperature as measured in the experiment. Instead, we can only calculate and compare the triplex electrostatic free energies for the different sequences.

First, the TBI-predicted sequence-dependent stability of DNA triplex agrees with the experimental results. Second, in general, the results show that sequences with more C^+C triplets are more stable. Physically, the positive charge on the C^+ can partially overcome the charge repulsion of negative charges in phosphates and help to bring the strands together by attracting the negatively charged phosphates on the other strands. This would help lower the electrostatic free energy of the system and stabilize the triplex structure; see figure 8(*B*). As a result, the melting temperature is increased, see figure 8(*A*).

In addition, we find that the TTT triplex is more sensitive to the ionic strength than the other triplexes. The sensitivity to ionic strength depends on the proportion of T·AT. Sequences with a greater number of C^+C triplets are less sensitive to changes in the ionic conditions. As a result, the CTCT triplex is the most stable triplex, while the TTT is the least stable triplex. This is due to the positive charge on the C^+ (protonated cytosines), which can partly overcome the negative charges in the phosphates, which results in a lower net charge density in the triplex. The triplex with lower charge density involves weaker ion–helix interactions and hence less sensitivity to changes in the ion conditions.

When the ion concentration is low, charge neutralization is not significant; therefore, the free energy and the melting temperature are more sensitive to the ion concentration. When the ion concentration is high, the sharp decrease of electrostatic free energy with the increase of Mg^{2+} would slow down. This is because when $[Mg^{2+}]$ is high enough, the triplex is almost fully neutralized and the decrease in electrostatic free energy caused by further addition of ions is saturated.

We also find that the inter–helix interaction is dependent on the sequence length. The inter-axial spacing increases with the decrease of triplex length (see figure 7(*B*)). For larger triplex length N, the electric field near the helix surface is stronger, attracting more ions to bind to the helices and causing a lower free energy minimum. Therefore, the equilibrium inter-helix distance $\bar{x}$ decreases with the increase of triplex length.

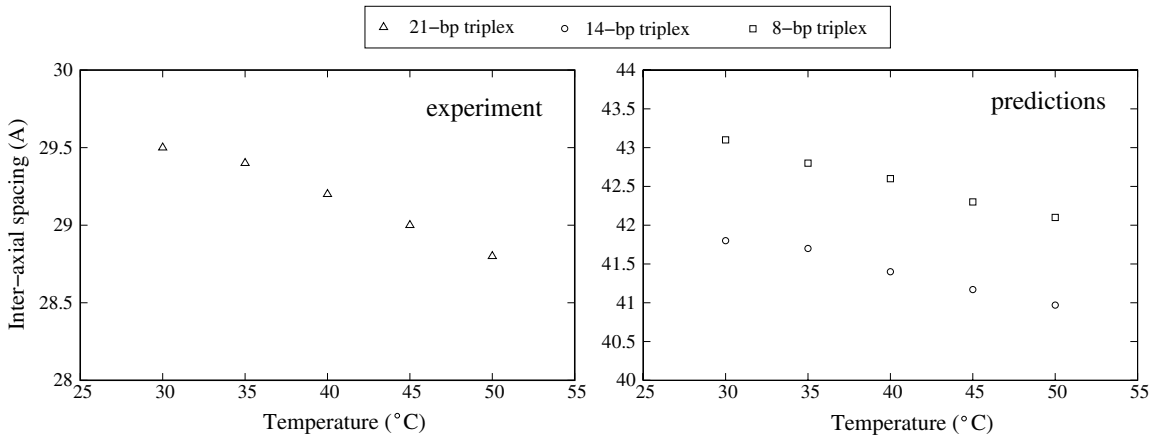

Figure 7. Temperature dependences of inter-axial spacings of two parallel tsDNA in 0.05 M Mg^{2+}. The experimental data are taken from [9].

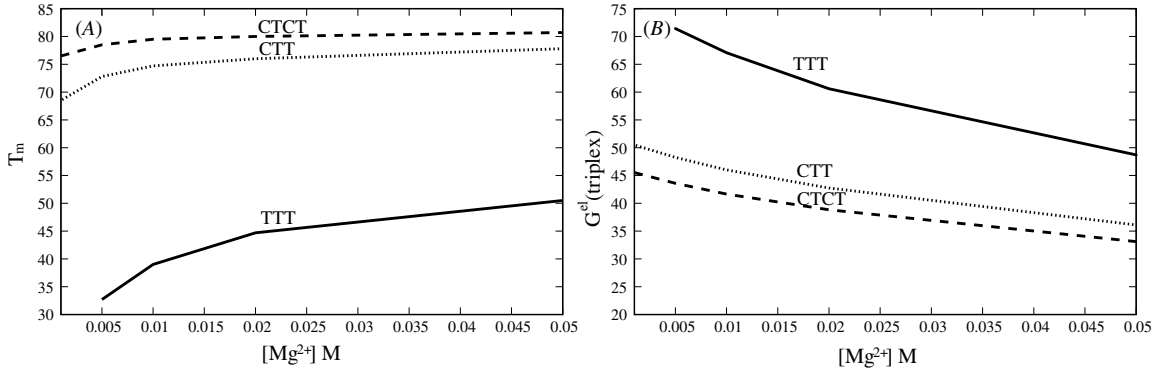

Figure 8. The sequence and ion-dependent stability of DNA triplexes. (*A*) The experimental results for the ion effect on the melting temperatures of the three intermolecular triplexes [10]. (*B*) Theoretically predicted triplex electrostatic free energy of the three intermolecular triplexes at 25°C. Following the experimental condition, we assume a solution of 50 mM NaCl and pH 5.0.

Conclusions and discussions

Using an extended TBI theory to account for the correlations and fluctuations of the ion distribution, we investigate the ion-dependent stability for a series of experimentally studied systems such as a 24-base DNA triplex in Mg^{2+} solutions. Our TBI model-predicted number of bound ions agrees with the experimental results. We also calculate the stability of a pair of 14-mer triple helices immersed in Mg^{2+} solutions and the sequence-dependent stability of 15-base DNA triplexes. The comparisons between the theoretical predictions and the experimental data lead to several conclusions on the ion-mediated triplex stability.

(1) PB underestimates the number of Mg^{2+} ion binding to a DNA triplex and overestimates the number of Na^{+} ion binding. The TBI model gives much improved predictions than PB for the number of bound ions.
(2) Ion correlation may be more important for a triplex than for a duplex.
(3) Divalent cations can condense tsDNA at millimolar concentrations, and the attraction between two helices increases with the increase of ion concentration.
(4) The predicted inter-axial spacing of two parallel tsDNAs decreases with the increase of the temperature. The result is consistent with the experiment.
(5) Sequences with more $C^{+}C$ triplets are generally more stable than sequences with less $C^{+}C$ triplets. The sensitivity to ionic strength depends on the proportion of $C^{+}C$ triplets in a triplex. Sequences with a larger number of $C^{+}C$ triplets are less sensitive to changes in the ionic conditions.

Our theoretical modeling here has several limitations owing to the use of simplified approximations. First, we have neglected the possible specific site binding of the ions in the tightly bound region [17–19]. Specific ion-binding could affect the ion distribution and thus influence the electrostatic interactions. Although the overall contribution from a small number of specific bound ions to the global inter-triplexes interaction might not be significant, thorough examination is required to quantitatively evaluate the contribution from the specifically bound ions. Second, although the model uses the GB theory for the solvent effect, it may not be able to provide a detailed accurate treatment for the possible ion dehydration and polarization effect, which could be an important source for the ion-mediate attraction between the triplexes [20, 21]. Third, the current TBI theory does not explicitly consider the effect of anions in the tightly bound region. The bound anions may become important at very high salt concentrations [22–24]. This might also contribute to the theory–experiment

differences for high salt concentrations. Finally, in the landscape calculation, we use much shorter triplexes than the ones used in the experiment. Future development of the model should aim to treat longer and more complex nucleic acid structures with considerations of site-binding of ions, the dehydration effect and the effect from the anions in the solution.

Acknowledgments

This research was supported by NSF through grants MCB0920067 and MCB0920411 and by NIH through grant GM063732. Most numerical calculations involved in this research were performed on the HPC resources at the University of Missouri Bioinformatics Consortium (UMBC).

References

[1] Felsenfelda G and Richa A 1957 Studies on the formation of two- and three-stranded polyribonucleotides *Biochim. Biophys. Acta* **26** 457–86
[2] Majumdar A *et al* 1998 Targeted gene knockout mediated by triple helix forming oligonucleotides *Nat. Genet.* **20** 212–14
[3] Maxim D and Sergei M M 1995 Triplex DNA structures *Annu. Rev. Biochem.* **64** 65–95
[4] Barawkar D A, Rajeev K G, Kumar V A and Ganesh K N 1996 Triplex formation at physiological pH by 5-Me-dC-N4-(spermine) [X] oligodeoxynucleotides: non-protonation of N3 in X of X*G:C triad and effect of base mismatch/ionic strength on triplex stabilities *Nucleic Acids Res.* **24** 1229–37
[5] Coman D and Russu I M 2004 Site-resolved stabilization of a DNA triple helix by magnesium ions *Nucleic Acids Res.* **32** 878–83
[6] Lavellea L and Fresco J R 2003 Stabilization of nucleic acid triplexes by high concentrations of sodium and ammonium salts follows the Hofmeister series *Biophys. Chem.* **105** 681–99
[7] Bai Y, Greenfeld M, Travers K J, Chu V B, Lipfert J, Doniach S and Herschlag D 2007 Quantitative and comprehensive decomposition of the ion atmosphere around nucleic Acids *J. Am. Chem. Soc.* **129** 14981–88
[8] Bloomfield V A 1997 DNA condensation by multivalent cations *Biopolymers* **44** 269–82
[9] Qiu X, Parsegianb V A and Donald C R 2010 Divalent counterion-induced condensation of triple-strand DNA *Proc. Natl Acad. Sci. USA* **107** 21482–6
[10] James P L, Brown T and Fox K R 2003 Thermodynamic and kinetic stability of intermolecular triple helices containing different proportions of C^+GC and T.AT triplets *Nucleic Acids Res.* **31** 5598–606
[11] Tan Z J and Chen S J 2005 Electrostatic correlations and fluctuations for ion binding to a finite length polyelectrolyte *J. Chem. Phys.* **122** 044903
[12] Chen S J 2008 RNA Folding: conformational statistics, folding kinetics *Annu. Rev. Biophys.* **37** 197–214
[13] Chen G S, Tan Z J and Chen S J 2010 Salt-dependent folding energy landscape of RNA three-way junction *Biophys. J.* **98** 111–20
[14] Ferro D R and Hermans J 1971 A different best rigid-body molecular fit routine *Acta Crystallogr.* **A33** 345–47
[15] Tan Z J and Chen S J 2008 Electrostatic free energy landscape for DNA helix bending *Biophys. J.* **94** 3137–49
[16] Ivanov S, Alekseev Y, Bertrand J R, Malvy C and Gottikh M B 2003 Formation of stable triplexes between purine RNA and pyrimidine oligodeoxyxylonucleotides *Nucleic Acids Res.* **31** 4256–63
[17] Tan Z J and Chen S J 2006 Nucleic acid helix stability: effects of salt concentration, cation valency and size, and chain length *Biophys. J.* **90** 1175–90
[18] Stellwagen E, Dong Q and Stellwagen N C 2007 Quantitative analysis of monovalent counterion binding to random-sequence, double-stranded DNA using the replacement ion method *Biochemistry* **46** 2050–58
[19] Lu Y and Stellwagen N C 2008 Monovalent cation binding by curved DNA molecules containing variable numbers of a-tracts *Biophys. J.* **94** 1719–25
[20] Draper D E, Grilley D and Soto A M 2005 Ions and RNA folding *Annu. Rev. Biophys. Biomol. Struct.* **34** 221–43
[21] Rau D C and Parsegian V A 1992 Direct measurement of the intermolecular forces between counterion-condensed DNA double helices. Evidence for long range attractive hydration forces *Biophys. J.* **61** 246–59
[22] Chen A A, Marucho M, Baker N A and Pappu R V 2009 Simulations of RNA interactions with monovalent ions *Methods Enzymol.* **469** 411–23
[23] Chen A A, Draper D E and Pappu R V 2009 Molecular simulation studies of monovalent counterion-mediated interactions in a model RNA kissing loop *J. Mol. Biol.* **390** 805–19
[24] Chen A A and Pappu R V 2007 Quantitative characterization of ion pairing and cluster formation in strong 1:1 electrolytes *J. Phys. Chem. B* **111** 6469–78